

Adapted Surface Visualization of Cerebral Aneurysms with Embedded Blood Flow Information

Rocco Gasteiger^{*1}, Mathias Neugebauer¹, Christoph Kubisch¹, Bernhard Preim¹

¹Department of Simulation and Graphics, University of Magdeburg, Germany

Abstract

Cerebral aneurysms are a vascular dilatation induced by a pathological change of the vessel wall and often require treatment to avoid rupture. Therefore, it is of main interest, to estimate the risk of rupture, to gain a deeper understanding of aneurysm genesis, and to plan an actual intervention, the surface morphology and the internal blood flow characteristics. Visual exploration is primarily used to understand such complex and variable type of data. Since the blood flow data is strongly influenced by the surrounding vessel morphology both have to be visually combined to efficiently support visual exploration. Since the flow is spatially embedded in the surrounding aneurysm surface, occlusion problems have to be tackled. Thereby, a meaningful visual reduction of the aneurysm surface that still provides morphological hints is necessary. We accomplish this by applying an adapted illustrative rendering style to the aneurysm surface. Our contribution lies in the combination and adaption of several rendering styles, which allow us to reduce the problem of occlusion and avoid most of the disadvantages of the traditional semi-transparent surface rendering, like ambiguities in perception of spatial relationships. In interviews with domain experts, we derived visual requirements. Later, we conducted an initial survey with 40 participants (13 medical experts of them), which leads to further improvements of our approach.

Categories and Subject Descriptors (according to ACM CCS): I.3.7 [Computer Graphics]: Visible line/surface algorithms, I.3.3 [Computer Graphics]: Line and Curve Generation, I.3.7 [Computer Graphics]: Color, shading, shadowing, and texture

1. Motivation

The treatment of frequent vascular diseases, such as cerebral and abdominal aneurysms aims at correcting blood flow in a specific way. CFD simulations of blood flow for different treatment variants have the potential to strongly improve treatment decisions and disease understanding [HMWea04, CCA*05]. However, the complex vascular anatomy has to be visualized along with the internal flow simulations results. Since the blood flow data is strongly influenced by the surrounding vessel morphology both information have to be visualized in an embedded surface rendering in order to efficiently support the visual exploration process. To visualize multiple superimposed layers of information, embedded surface rendering techniques are used to reveal internal information by resolving occlusions appropriately. A trade-off

between the visibility of internal information and the simultaneous depiction of the three-dimensional shape of the enclosing surface has to be found.

Near-wall flow characteristics like wall shear stress (WSS), can be displayed with a combined map-to-surface approach [NGB*09]. However, when visualizing the internal flow information, we have to cope with the aforementioned occlusion problems. A common approach is to render the enclosing surface semi-transparently. More transparency increases the visibility of the internal flow visualization. As a consequence, necessary depth cues to depict the aneurysm surface shape get strongly reduced. Additionally, regions, where several layers of semi-transparent surfaces lie in front of each other, can cause a misleading interpretation of spatial relationship. Both problems decrease the observers ability to mentally link the aneurysm morphology with the internal flow data.

^{*}rocco@isg.cs.uni-magdeburg.de

We aim at an adapted visualization of the enclosing aneurysm surface, that depicts important morphological features, whilst simultaneously gaining maximal visibility of the embedded flow visualization. The definition of what is such an "important" feature, was derived from discussions with neuroradiologists. Our approach is inspired by illustrative visualization techniques like line rendering and ghosted views. These techniques are used in traditional illustrations for conveying shape and surface features as well as preserving visibility of embedded surfaces. Additionally, we employ atmospheric attenuation and shadow casting as to increase perception of depth and spatial relationship. These design decisions are inspired by other medical applications, e.g., liver surgery and neck dissection [PT06, TPB*08].

We conducted an initial survey with domain experts (40 participants, among them 13 medical experts). We presented visualizations of different types of cerebral aneurysms that include internal blood flow depiction. The participants had to compare our approach with a common semi-transparent surface rendering. The survey indicates that our approach increased perception of blood flow tracing. However, perception of shape and spatial relationships was partially rated as poor. This insight was used to improve our approach.

The paper is organized as follows: we first briefly discuss the medical background in Sec. 2 and describe related work in Sec. 3. We discuss the underlying data and conduct a requirement analysis for embedded surface rendering of cerebral aneurysms with internal flow in Sec. 4. Based on these requirements, the conceptual design and implementation details are described in Sec. 5. Our initial domain expert survey, its findings, and resulting improvements for our approach are presented in Sec. 6 and Sec. 7. We conclude our work with an outlook on future work in Sec. 8.

2. Medical Background

Cerebral aneurysms result from a congenital or evolved weakness of stabilizing parts of the vessel wall and leads to a local dilatation. The affected area bears a high risk of rupture with often fatal consequences for the patient (fatality up to 52%) [JPP00]. Due to an increase of performed MR scans, the number of accidentally found aneurysms is rising. Together with the internal flow characteristics, the surface morphology of the aneurysm plays an important role in the risk assessment process [VMM05]. The most important morphological features were derived from discussions with neuroradiologists (see Fig. 1):

- Inflow and outflow region
- Aneurysm sack and ostium
- Presence of satellites on the aneurysm (high local bulge on the aneurysm, indicating a former bleeding)

Qualitative and quantitative analysis of these features convey relevant information for estimating the aneurysm's condition, the risk of rupture, and options for treatment plan-

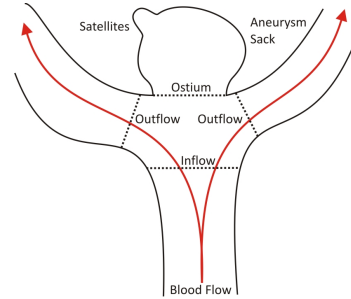


Figure 1: Illustration of important morphological features of a cerebral aneurysm.

ning. However, aneurysms often rupture although morphologic criteria did not reveal an increased risk. To better support the decision-making process and disease understanding, current medical research aims at additional information derived from computational fluid dynamic (CFD) simulations of the intravascular blood flow [CCA*05]. Based on the geometrical mesh of the aneurysm a finite element method (FEM) mesh is build and a specific blood flow model is applied to it. The results contain several hemodynamic information like flow direction, velocity, pressure, and WSS.

3. Related Work

Embedded surface rendering is important in medical research and treatment, for example in radiation therapy treatment planning [IFP97], liver surgery planning [PT06], or biomedical problems like visual exploration of nasal air-flow [ZMH*09]. Similar to the visual exploration of hemodynamic data in cerebral aneurysms, a semi-transparent rendering of the enclosing surface is used, faced with the same challenges according to shape and depth perception. More transparency increases the visibility of the internal flow visualization. However, with strong transparency, details of surface shape, like small satellites on the aneurysm are difficult to recognize. Moreover, regions of self-occlusions lead to misleading interpretation of spatial relationships. For example, it is difficult to verify, which parts of the vessel are in front or behind to each other if transparency is high, especially for static images. Additionally, flow quantities like velocity are often mapped on visual attributes (e.g., color). A semi-transparent layer in front of the flow visualization can mislead the interpretation of the flow quantity.

Inspired by artistic line drawings, Interrante et al. [IFP97] investigated how sparsely-distributed opaque texturing can be used for conveying shape. They apply principle direction texture stripes on the enclosing surface and show that its 3D shape and relative depth to the embedded object can be more easily and accurately perceived. Similar approaches exist to depict the 3D shape by employing illustrative line renderings with contour rendering as well as more sophisticated

approaches, such as suggestive contours and apparent ridges (DeCarlo et al. [DFRS03] and Judd et al. [JDA07]). These methods aim at reproducing artistic line drawings based on differential surface properties and achieve a reduced surface description as well as visual pleasant results. Recent studies from Cole et al. [CSDea09] confirm its applicability. Several medical applications like intervention planning or training adopt these approaches to convey context information, depth cues or spatial relationships [PT06, RHD*06]. Although line rendering and sparsely-distributed texturing achieve a sufficient surface description, they are not optimal for surface rendering of vascular structures with internal flow. Especially curvature-based methods generate lines (or stripes) on the surface, which yield a cluttered result for the visual exploration of the internal blood flow behind.

Smart visualization techniques are also used for visualizing multiple superimposed layers of information. They focus on exposing the most important visual information in the resulting images. Smart visibility techniques originate from technical illustration. Examples are cut-away views, ghosted views, section views, and exploded views. Viola and Gröller discuss these techniques, which are also applicable for intervention planning and disease understanding [VG05]. The basic strategy of these "smart" techniques is to emphasize the most relevant visual information of an object by means of local modifications of visual representations or changes in spatial arrangement according an importance value of the object. In our application, we define the internal flow as most important visual information. Since exploded views decrease the observers ability to mentally link the aneurysm morphology with the internal flow data, we adopt techniques with local modifications of visual representations. Similar problems occur for masking techniques like cut-away and section views. Since they perform a view-aligned local clipping of enclosing surface parts all morphological information related to local internal structures (e.g., flow) are lost. Similar color modifications are also performed in illustrative volume rendering for flow, science, and medicine by means of "smart" transfer functions [SJEG05, GOHea10]. Our approach is also related to conveying depth information and spatial relationships. Several approaches employ advanced shading techniques to address these issues [LCD06]. Medical applications of these techniques can be found in [DWE03, TPB*08].

4. Data Basis and Requirement Analysis

Since surface morphology and hemodynamic influence one another, domain experts are interested in an embedded visualization of both information. We briefly describe the steps necessary to provide the needed data before analyzing the requirements for a comprehensible visualization of vessel morphology and the internal blood flow. Based on the requirements, we describe our approach. The data flow pipeline consists of three processes, illustrated in Fig. 2.

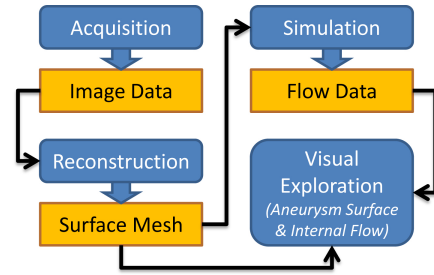


Figure 2: Data flow for visual exploration purposes of blood flow in cerebral aneurysms.

4.1. Data Flow Pipeline

In the acquisition step, clinical image data (MRA, CTA, or 3DRA) of the aneurysm is obtained. Because of the high vessel contrast we are able to use a simple thresholding followed by a connected component analysis to separate the aneurysm and its parent vessel from the surrounding tissue. Manual effort is only necessary to define a region of interest around the aneurysm (mainly to exclude bone structures) and in rare cases to mask beam hardening artifacts. More advanced techniques like model-based approaches can be employed to minimize manual effort in cases of low intensity distribution [HF07]. The overall segmentation time takes about 10 minutes for most of our clinical datasets. Based on the segmented mask, the surface morphology of the aneurysm is reconstructed and optimized with respect to mesh quality [CCA*05]. The resulting mesh is used for constructing a computational grid, on which a CFD simulation is performed. Regarding the resulting blood flow data, we only consider internal flow information. According to the morphological features (recall Sec. 2) we currently extract them in a manual preprocessing step. We define deformable cutting planes at each individual feature and intersect them with the aneurysm morphology. This yield disc-like mesh structures which are the union of the the cut planes with the intersected regions. Depending on the number of existent features the manual extraction needs about 10 minutes for each dataset. The surface mesh, morphological features, and the blood flow data form the input for the final visual exploration. In the following, we discuss the requirements that need to be met in order to efficiently support the qualitative analysis during this process.

4.2. Requirement Analysis

A detailed visual description of the enclosing surface leads to an increased occlusion of internal information. Thus, an adapted surface visualization is needed to decrease the occlusion problem. Based on the previous discussions with our domain experts, we address the following requirements:

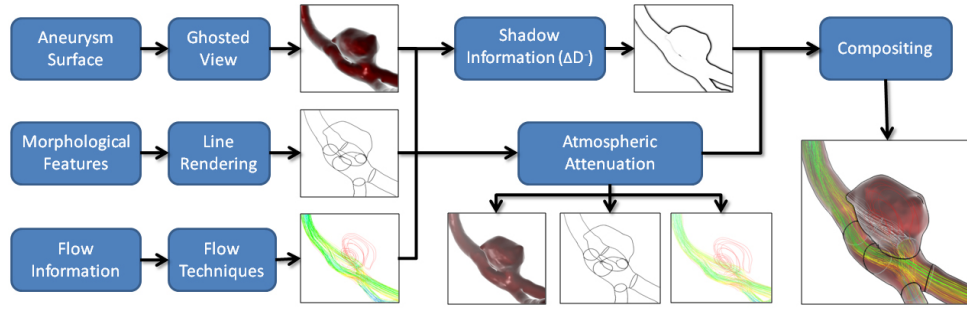


Figure 3: Overview of our adaptive surface visualization approach: we apply illustrative rendering styles to the aneurysm surface, its shape and morphological features. Flow information is visualized with established visualization techniques. All resulting images receive an atmospheric attenuation and are composed with shadow information to the final visualization.

Visibility of Internal Flow Information: A maximum visibility of the internal flow visualization is required during the visual exploration and qualitative evaluation process. With "maximum visibility", we mean as few as possible occlusion of the flow visualization. This supports the viewer in interpreting and tracing the flow.

Depicting Aneurysm Features and Surface Shape: The morphological features of the aneurysm, described in Sec. 2 have to be depicted. Together with the boundaries of the vessel morphology, these features form the "skeleton" of the aneurysm morphology. This involves enhancement of surface regions with high curvature to indicate satellites.

Spatial Relationships and Depth Cues: Occluded morphological surface features and flow information have to be distinguished from visible parts of the surface and flow. Additionally, depth cues according to overlapped vessel parts and surface distances to the viewer have to be provided. These hints increase perception of spatial relationships between different vessel parts and tracing the internal flow. Furthermore, attenuation of distant information, supports focusing on relevant information close to the viewer.

5. Adapted Surface Visualization

We achieve an adapted surface visualization by composing several illustrative rendering styles, shown in Fig. 3. As input, we employ the aneurysm surface (as a mesh), its morphological features (a subset of the mesh), and internal flow information (represented as vector data). A ghosted view is applied to the aneurysm surface and line rendering is used to depict shape and morphological features. Flow information is visualized with established visualization techniques. Each of these rendering styles receives an atmospheric attenuation to enhance spatial perception. In a last step, all individual styles are composed with shadow information to the final visualization. In the following, we give a detailed description of each stage.

5.1. Ghosted View

Inspired by smart visibility techniques, we define flow as most important visual information and the enclosing surface as less important. We achieve "smart" visibility by applying a ghosted view to the front faces by means of a view-dependent transparency rendering. We employ an approximation of Fresnel-reflection model [Sch93] and replace "reflection" with "opacity", with dark \triangleq low opacity and bright \triangleq high opacity, shown in Fig. 4(a). The Fresnel opacity F_O can be expressed as $F_O = 1.0 - (|N \bullet V|)^r$, where N is the surface normal, V is the view vector, and r is a user specified edge fall-off parameter ($r \geq 0$). We linearly blend between front and back face color controlled by F_O , depicted in Fig. 4(b). As a result, we achieve more opacity at regions facing away from the viewer and more visibility at regions facing to the viewer.

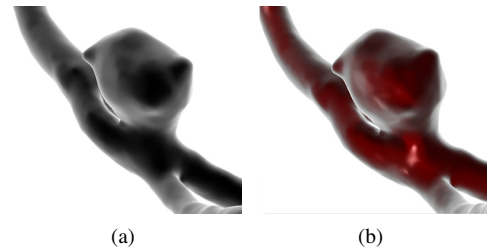


Figure 4: The Fresnel opacity (a) modifies the front face opacity to yielding a ghosted view on the back faces (b).

5.2. Line Rendering

As an established technique to convey shape, line drawings are used [CSDea09]. During interviews and discussions with domain experts, we noticed that they used line drawings for the aneurysm shape and its features. Since, line rendering seems to be an intuitive way to communicate information,

we investigate contours to depict morphological features (recall Sec. 2). We do not use curvature-based line rendering like suggestive contours or apparent ridges, as they introduce disturbing information on the vessel surface due to the sensitivity regarding the surface curvature. Resulting images of both techniques are presented in Fig. 5(a) and (b)*.

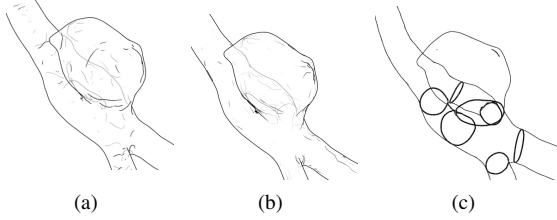


Figure 5: In comparison to suggestive contours (a) and apparent ridges (b), simple contour rendering depicts aneurysm shape and features (thick lines) more clearly (c).

However, these lines degrade perception of internal flow information, especially if streamlines are used. Thus, we restrict line rendering to contours and morphological features, which results in a clear description of the aneurysm, presented in Fig. 5(c). We implement the object-based line rendering approach of McGuire and Hughes [MH04] to achieve interactive frame rates and individual line stylization, e.g., stippling patterns or texturing. Image-based approaches are less flexible concerning the control over resulting line attributes [IFH*03]. Furthermore, we perform two line rendering passes, each with a different line style used in the compositing to distinguish between visible and hidden lines.

5.3. Flow Visualization

The internal blood flow information consists of vector information and more complex flow features, like vortices or other critical points. A large variety of techniques exists to visualize these information [LHD*04]. We consider only visualization techniques frequently used for visualizing blood flow, like streamlines, glyphs, or stream surfaces [CCA*05].

5.4. Shadow

Shadow is an important depth cue. To increase depth perception between overlapped vessel parts, we employ shadow casting. We approximate this effect in a non-physical correct way, by applying the method of Luft et al. [LCD06]. They compute a function ΔD from the depth buffer and its low-pass filtered version. The original image is then modified with ΔD^- (see Fig. 3) to cast shadow on the objects background. We apply this approach for the depth buffer of

the vessel front faces. However, we modify the computation of the depth buffer values. Depth values correspond to object distances related to the camera's near and far clipping plane. If these planes will change, e.g., due to zooming (perspective camera) or translation (orthographic camera), resulting depth values also change. This causes a non constant appearance of the shadow casting in screen space, resulting in a misinterpreting of spatial distances. Since, camera zooming is an important interaction scheme during the visual exploration process constant depth cue appearance is necessary. Additionally, to resolve the precision issue of original depth buffering (logarithmic scale), we perform a computation of linear depth values in the vertex shader, presented in Algorithm 1.

Algorithm 1 Depth Computation

Input:

AABB Axis Aligned Bounding Box of the aneurysm

C Center of **AABB**

P Camera position

Output:

 Linear depth value d_v for each vertex v

```

1: for Each Frame do
2:    $s$  = view vector between P and C
3:    $n_i$  = normal at corner  $c_i$  of AABB
4:    $\alpha_i$  = angle between  $s$  and  $n_i$ 
5:    $c_i$  = smallest  $\alpha_i$ 
6:    $c_j$  = diagonal corner of  $c_i$ 
7:    $near = d(P, c_i)$  and  $far = d(P, c_j)$ 
8:    $d_v = 1.0 - \frac{(far - v_z)}{(far - near)}$ 
9: end for

```

In line 7 the values *near* and *far* represent minimum and maximum depth values in eye space. They are expressed as distances of *P* between c_i and c_j . Both values are computed in the functions $d(P, c_i)$, $d(P, c_j)$, and delegated to the vertex shader to compute d_v .

5.5. Atmospheric Attenuation

In addition to shadow casting, we perform atmospheric attenuation as second depth cue. According to our requirements, these hints support the viewer in tracing the flow as well as focusing on close visual information. Attenuation is introduced by applying fog to the previous visual representations, which makes the objects fade into the distance d_v from Algorithm 1. Because flow attributes, like velocity or pressure, are often color coded, color modifications are not appropriate, since it can cause a misleading interpretation of the coded attribute. The resulting attenuation can be seen in the final composed visualization of Fig. 3.

5.6. Compositing

The previous stages of our approach result in several off-screen rendered images. Additionally, we rendered a linear

*Surface renderings of 5(a) and (b) are generated with the software `rtcs`, provided on the website of Judd et al. [JDA07].

depth buffer for each colored object, according to d_v . We use following images as input textures in a final full screen compositing pass:

- front and back faces (color and depth)
- contour, feature and hidden lines (color and depth)
- shadow information ΔD^- (color)
- flow visualization (color and depth)

The depth information control visual appearance of hidden regions. This concerns line rendering for depicting shape and morphological features as well as flow information.

6. Domain Expert Survey

To get feedback from our target user group, we conducted an initial domain expert survey with 40 participants (13 of which were medical experts). Based on this survey, we got important findings to improve the perception. These improvements are then integrated in our approach.

Survey Design: We designed a web-based questionnaire, which contains 30 randomized image pairs. One web page for each image pair. Each pair consists of one of three aneurysm surface renderings one depicting semi-transparently (50% transparency) and one with our approach. Camera settings are identical for each individual pair but changed between two pairs. Light conditions are constant. Furthermore, colored streamlines depict internal flow information for each aneurysm dataset. We evaluate our approach according to four criteria with following questions:

- **Depth Perception:** "Which figure conveys more information about depth?"
- **Spatial Relationships:** "In which figure you can recognize more overlapping surface parts?"
- **Flow Perception:** "In which figure you can better perceive the flow?"
- **Surface Shape:** "In which figure you can recognize the surface shape better?"

For each question, the participant was prompted to decide between one of the two images. Additionally, each subject had to rate its medical experience and had the opportunity to provide a comment at the end of the questionnaire.

7. Results and Discussion

We applied our approach to several clinical datasets, which represent not only standard types of cerebral aneurysms but also special cases (e.g., presence of satellites, rare forms of bifurcations). To create the surface (up to 72.218 faces) and simulation data, we applied the pipeline described in Sec. 4.1. The presented algorithms have been realized with VTK and GLSL utilizing multiple render targets to reduce the number of render passes. On a standard PC (3.2 GHz Core Duo, 4GB RAM) using a NVIDIA GeForce 9800 GT, we achieve interactive-frame rates for a screen resolution

of 1280×1024 . We provide empirical default values for the user-defined parameters. User interaction is only necessary to turn-on/off individual render layers (e.g., hidden lines).

In Fig. 7, we present a comparison between a semi-transparent visualization (Fig. 7(a)) and our approach (Fig. 7(b)) applied to an aneurysm dataset with colored streamlines. Our approach includes the depiction of inflow and outflow regions and emphasizes hidden surface parts and streamlines (colored in gray). The occlusion of the streamlines is reduced due to the ghosted view. Thus, the observer can track the flow more comprehensibly. Atmospheric attenuation and shadow casting improves depth perception compared to the semi-transparent visualization. However, due to the bright edge fall-off color the orientation of details on the enclosing surface, might be misinterpreted. This was reflected in the results of the initial survey.

7.1. Survey Results

For each criteria, we evaluate the participant's grade of satisfaction, as presented in Fig. 6. If a participant favored our

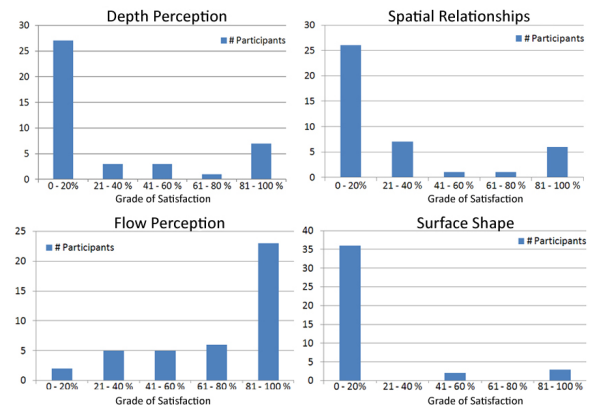


Figure 6: Survey results according to grade of satisfaction related to perception of depth, spatial relationships, flow, and shape.

approach for each of the 30 presented image pairs, his grade of satisfaction would be 100%, whereas a complete rejection results in a grade of 0%. It turns out, that most of the participants assessed our approach poorly related to perception of depth, spatial relationship, and surface shape. Especially in the case of shape perception, where 36 participants (90%) preferred our adapted visualization only to 20%. However, about 56% of participants favored our approach to 80-100% according to the perception of internal flow, compared to the semi-transparent visualization.

In addition to the statistic results, 54% of the participants have stated comments at the end of the questionnaire. In

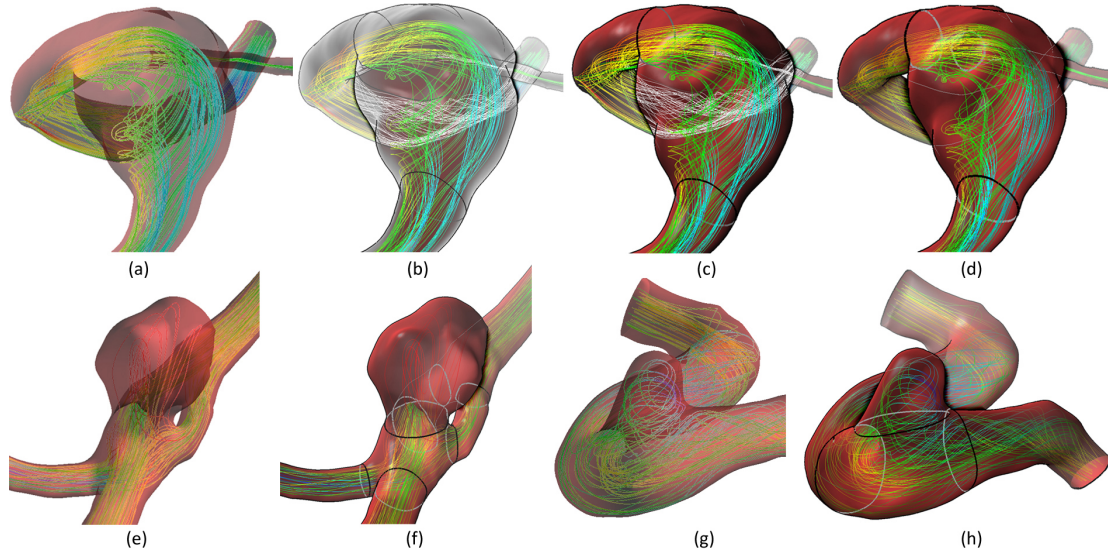


Figure 7: Comparison between a semi-transparent visualization (a) and our approach (b) applied on an aneurysm surface with color coded streamlines. Improved shape perception is achieved due to a dark edge fall-off color and distinguishable line rendering (c). Flow perception is increased by removing hidden flow information (d). Surface details, like high local bulges (satellites) are enhanced (f) in contrast to the semi-transparent visualization (e). Another dataset is shown in (g) and (h).

most comments, atmospheric attenuation and shadow casting were assessed helpful. Display of hidden surface parts and flow were assessed confusing and disturbing in some cases. In combination with streamlines, this results in an overloaded visualization.

7.2. Discussion and Consequences

Our adapted surface visualization is applicable to several clinical datasets with different grade of complexity. Currently, manual effort is needed in the preprocessing step mainly in extraction of the morphological features. Thus, we are investigating a semi-automatic approach to reduce user-interaction and preprocessing time. We consider information about the vessel centerlines and its local distances to the surrounding aneurysm surface. However, a detailed description is behind the scope of this paper and is left open for future work. Because of this limitation and due to the complex and not yet validated CFD simulations (a problem for most biomedical simulations) our approach is applicable to pretreatment discussions rather than clinical usage.

According to the survey, most of the criticisms were related to the inverted shading (recall Sec. 5.1 and Fig. 7(b)). The "unnatural" shading of areas facing away from the observer led to an inverted interpretation of the surface orientation. This confusion was increased due to the white background and the white atmospheric attenuation color. To gain more details, some of the participants were asked to interact with the visualization rather than looking at static images, with the result that the shading was now interpreted in

a correct manner and the feedback was much more positive. From this, we derive that the shading is appropriate for interaction purposes. However, for the usage in static depiction, we adopt our approach to a diffuse shading, resulting in dark edge fall-off color and increased shape description at these edges (see Fig. 7(c)).

Other comments criticized the undifferentiated thickness of the contour and feature lines as well as depicting the hidden flow information. Therefore, we increased the line width for morphological features and decreased the line width for visible and hidden contour lines, shown in Fig. 7(c) and (d). Additionally, hidden flow information is removed, in Fig. 7(d). In Fig. 7(e)-(g), we applied the altered version of our approach to a dataset, which consists satellites on the aneurysm surface (recall Sec. 2). In contrast to the semi-transparent visualization (Fig. 7(e)), high local bulges are more enhanced with our approach (Fig. 7(e)). Another dataset (without satellites) is shown in Fig. 7(g) and (h).

8. Conclusion and Future Work

We described an adapted visualization of cerebral aneurysm surfaces to expose embedded flow information. We employ line rendering for depicting aneurysm shape and morphological features as well as a ghosted view to reduce occlusion. Additionally, depth enhancement is achieved by means of shadow casting and atmospheric attenuation. Our approach is not restricted to cerebral aneurysms. In general, it can be applied to tubular structures with embedded information.

Our initial survey with 40 participants demonstrated a better perception of the embedded flow in comparison to a common semi-transparent surface visualization. Poor perception of shape, depth, and spatial relationships of the enclosing surface was caused by the inverted surface shading. As it turned out, this shading is more appropriate for interaction purposes than for static depiction. As a consequence, we altered the shading to achieve a dark edge fall-off. To increase spatial perception, we differentiated the line thickness of morphological features and hidden lines.

Based on the altered version, we will perform a second and more detailed follow-up survey. Thereby, we will focus on the suitability depending on the viewpoint, embedded flow visualization technique, and exploration task. Finally, investigations according to a semi-automatic extraction of the morphological aneurysm features is remaining.

Acknowledgment: We would like to thank V. Diehl (MR and PET/CT center Bremen) and O. Beuing (University Hospital Magdeburg) for providing clinical datasets and the fruitful discussions, G. Janiga and S. Seshadhri (ISUT Magdeburg) for providing the simulation data, A. Baer (ISG Magdeburg) for her help regarding the study design as well as all participants of the study for their patience and helpful comments.

References

- [CCA*05] CEBRAL J. R., CASTRO M. A., APPANABOYINA S., PUTMAN C. M., MILLAN D., FRANGI A. F.: Efficient Pipeline for Image-Based Patient-Specific Analysis of Cerebral Aneurysm Hemodynamics: Technique and Sensitivity. *IEEE Trans. Med. Imaging* 24, 4 (2005), 457–467.
- [CSDea09] COLE F., SANIK K., DECARLO D., ET AL.: How Well Do Line Drawings Depict Shape? In *ACM Transaction on Graphics (TOG)* (2009), vol. 28.
- [DFRS03] DECARLO D., FINKELSTEIN A., RUSINKIEWICZ S., SANTELLA A.: Suggestive Contours for Conveying Shape. *ACM Transactions on Graphics (TOG)* 22, 3 (2003), 848–855.
- [DWE03] DIEPSTRATEN J., WEISKOPF D., ERTL T.: Interactive Cutaway Illustrations. *Computer Graphics Forum* 22, 3 (2003), 523–532.
- [GOHea10] GLASSER S., OELTZE S., HENNEMUTH A., ET AL. B. P.: Automatic Transfer Function Specification for Visual Emphasis of Coronary Artery Plaque. *Computer Graphics Forum* 29 (1), 1 (2010), 191–201.
- [HF07] HERNANDEZ M., FRANGI A. F.: Non-parametric Geodesic Active Regions: Method and Evaluation for Cerebral Aneurysms Segmentation in 3DRA and CTA. *Medical Image Analysis* 11, 3 (2007), 224–241.
- [HMWea04] HOI Y., MENG H., WOODWARD S. H., ET AL.: Effects of Arterial Geometry on Aneurysm Growth: Three-Dimensional Computational Fluid Dynamics Study. *Journal of Neurosurgery* 101, 4 (2004), 676–681.
- [IFH*03] ISENBERG T., FREUDENBERG B., HALPER N., SCHLECHTWEIG S., STROTHOTTE T.: A Developer's Guide to Silhouette Algorithms for Polygonal Models. *IEEE Computer Graphics and Applications* 23, 4 (2003), 28–37.
- [IFP97] INTERRANTE V., FUCHS H., PIZER S. M.: Conveying the 3D Shape of Smoothly Curving Transparent Surfaces via Texture. *IEEE Trans. on Visualization and Computer Graphics (TVCG)* 3, 2 (1997), 98–117.
- [JDA07] JUDD T., DURAND F., ADELSON E. H.: Apparent Ridges for Line Drawing. *ACM Trans. on Graphics* 26, 3 (2007), 19–26.
- [JPP00] JUVELA S., PORRAS M., POUSSA K.: Natural History of Unruptured Intracranial Aneurysms: Probability of and Risk Factors for Aneurysm Rupture. *Journal of Neurosurgery* 93, 3 (2000), 379–387.
- [LCD06] LUFT T., COLDITZ C., DEUSSEN O.: Image Enhancement by Unsharp Masking the Depth Buffer. In *ACM Trans. on Graphics (TOG)* (2006), vol. 25, pp. 1206–1213.
- [LHD*04] LARAMEE R. S., HAUSER H., DOLEISCH H., VROLIJK B., POST F. H., WEISKOPF D.: The State of the Art in Flow Visualization: Dense and Texture-Based Techniques. In *Computer Graphics Forum* (2004), vol. 23, pp. 203–221.
- [MH04] MCGUIRE M., HUGHES J. F.: Hardware-Determined Feature Edges. In *Proc. of the 3rd International Symposium on Non-Photorealistic Animation and Rendering* (2004), pp. 35–47.
- [NGB*09] NEUGEBAUER M., GASTEIGER R., BEUING O., DIEHL V., SKALEJ M., PREIM B.: Combining Map Displays and 3D Visualizations for the Analysis of Scalar Data on Cerebral Aneurysm Surfaces. In *Computer Graphics Forum (EuroVis)* (2009), vol. 28, pp. 895–902.
- [PT06] PREIM B., TIETJEN C.: Illustrative Rendering for Intervention Planning: Methods, Applications, Experiences. In *Workshop on Eurographics* (2006).
- [RHD*06] RITTER F., HANSEN C., DICKEN V., KONRAD O., PREIM B., PEITGEN H.-O.: Real-Time Illustration of Vascular Structures. *IEEE Trans. on Visualization and Computer Graphics* (2006), 877–884.
- [Sch93] SCHLICK C.: A Customizable Reflectance Model for Everyday Rendering. In *Fourth Eurographics Workshop on Rendering* (1993), pp. 73–83.
- [SJEG05] SVAKHINE N. A., JANG Y., EBERT D. S., GAITHER K. P.: Illustration and Photography Inspired Visualization of Flows and Volumes. In *Proc. of IEEE Visualization* (2005), pp. 87–95.
- [TPB*08] TIETJEN C., PFISTERER R., BAER A., GASTEIGER R., PREIM B.: Hardware-Accelerated Illustrative Medical Surface Visualization with Extended Shading Maps. In *Proc. of SmartGraphics* (2008), pp. 166–177.
- [VG05] VIOLA I., GRÖLLER E.: Smart Visibility in Visualization. *Computational Aesthetics in Graphics, Visualization, and Imaging* (2005), 87–94.
- [VMM05] VINDLACHERUVU R., MENDELOW D., MITCHELL P.: Risk-Benefit Analysis of the Treatment of Unruptured Intracranial Aneurysms. *British Medical Journal* 76, 2 (2005), 234–239.
- [ZMH*09] ZACHOW S., MUIGG P., HILDEBRANDT T., DOLEISCH H., HEGE H.-C.: Visual Exploration of Nasal Airflow. *IEEE Trans. on Visualization and Computer Graphics (TVCG)* 15, 6 (2009), 1407–1414.